Numerical Investigation on Effect of Spark Plug Configuration on Performance in an Engine Cylinder

Bakhshi Mehul
Student
Department of Mechanical Engineering
K.K. Birla Goa Campus, BITS Pilani
India

Pritanshu Ranjan
Assistant Professor
Department of Mechanical Engineering
K.K. Birla Goa Campus, BITS Pilani
India

Anuj Kumar Shukla
Assistant Professor
Department of Mechanical Engineering
NIT Raipur
India

A numerical investigation of combustion inside single and twin-spark engines was performed to study the effect of a spark plug, positions and spark timings on engine performance. Improvement in engine performance is one of the automotive industry's primary research areas. Consequently, the study's results can be utilised to optimise engine configurations to achieve maximum performance. The investigation was conducted using a finite volume-based open-source software, OpenFOAM, for computational simulations. Simulations were conducted using the XiEngineFOAM solver with a transport equation for modelling flame fronts. The Standard k-ε turbulence model was used to predict turbulence parameters. The simulation was conducted for compression and power stroke (crank angle between -180° and 180°), assuming an even distribution of the air-fuel mixture within the pentroof 4-valve engine cylinder. Simulations were conducted for four cases, including variations in the position and timing of spark plugs in single-spark and twin-spark engines. According to the results of the simulations, the single-spark engine provides the best performance when the spark plug is ignited early and positioned at the cylinder's centre. When placed at an optimal position determined by flame travel and collision, the twin-spark engine gives the best performance at the highest difference between the spark timings of the two spark plugs.

Keywords: *OpenFOAM, premixed turbulent combustion, twin-spark, Kiva test, flame propagation, indicated power, PIMPLE.*

1. INTRODUCTION

The spark plug plays an important role in the ignition of the air-fuel mixture in an internal combustion engine. They convert the high-voltage electricity into an artificial bolt of lightning known as a spark, which paves the way to the initial ignition of the highly flammable air-fuel mixture. Since the invention of spark plugs, it has been widely used in engines and has also found some applications in industry to ignite fuel in furnaces, boilers and combustion chambers. The configurations of spark plugs, such as position and timing, can significantly impact engine performance. The timing of the spark plug can have an impact on the knock tendency and combustion duration, while the position of the spark plug can have an effect on the homogeneity and turbulence of the air-fuel mixture inside the engine cylinder.

The effect of spark plug parameters on engine performance has been investigated in a considerable number of past studies. Past research has demonstrated that a larger engine has a greater impact on spark plug placement than a smaller engine. When a spark plug was positioned in the centre of the engine cylinder [1, 2] or had a greater spark advance [3], peak pressure and reaction progression were observed to be higher. Research on the twin-spark engine has revealed that the position of the spark plug has little effect on the pressure regime [3]. However, for a direct injection methanol engine with a medium compression ratio, the greatest results were obtained with a 0.65 ratio between the distance of the twin spark plugs and the cylinder diameter [4]. An experimental investigation of a twin spark engine with three various ignition timings and load conditions determined that the same spark timings of the spark plugs resulted in the highest brake thermal efficiency, volumetric efficiency, and lowest CO and UBHC emissions [5]. There have been some other past studies as well, discussing the variation of spark plug position [6, 7], ignition timing [8, 9, 10] and flame front collision [11, 12] in twin spark engines within the engine cylinder. All of these past studies provides us with an understanding of how spark plug parameters can affect engine performance. However, we found a lack of literature that explicitly discusses together the variation of ignition position and timing through flame front propagation and interaction for single and twin spark plug engines.

The present investigation seeks to fill this gap in the literature by conducting numerical investigations on the effect of spark plug configurations on engine cylinder performance and a thorough comparison of the variations. Additionally, the research seeks to determine the optimal spark position and timing for both single and twin-spark engines and discuss the effect of flame front propagation and collision inside the cylinder. The

Received: June 2023, Accepted: September 2023
Correspondence to: Bakhshi Mehul, Department of Mechanical Engineering, K.K. Birla Goa Campus, BITS Pilani, India, E-mail: mehulbakhshi2@gmail.com
doi: 10.5937/fme2304585M

investigation was conducted using the simulation software OpenFOAM. Simulations were conducted to examine the impact of spark plug configurations on a variety of engine parameters, including in-cylinder pressure, in-cylinder temperature, indicated power, and flame propagation. As the automotive industry strives to satisfy increasingly stringent environmental regulations while also enhancing the performance and efficiency of internal combustion engines, this research is particularly pertinent today. By obtaining a deeper understanding of the effect of spark plug configurations on engine per–formance, it will be possible to identify spark plug con–figurations that concurrently improve engine perfor–mance and reduce emissions.

This paper will commence by describing the study's methodology, including simulation setup and validation. The paper will conclude with an analysis of the nume–rical simulation results, giving the optimal arrangement of spark plug positions and spark timings in an ideally homogenous charge for best results in both single and twin spark engines.

2. COMPUTATIONAL METHODOLOGY

2.1 Computational Domain and Engine Details

The pentroof-4-valve engine was used in the present study. This cylinder design has proved to be effective for fast burn time and producing high horsepower. The geometry is kept the same as that of the already present tutorial of XiEngineFOAM (Kiva Test) in OpenFOAM.

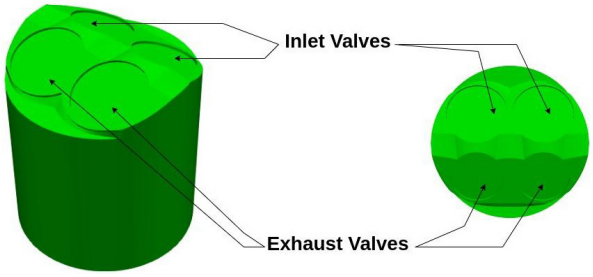

Figure 1. Isometric-view (left) and top-view (right) of exha–ust and inlet valves of pent-roof 4-valve engine.

The geometry has three boundary conditions, i.e. cylinder head, liner and piston [13], where the piston is moving with every time step, as depicted in Figure 2. Other details of the engine are mentioned in Table 1.

Table 1. Engine details

S. No.	Engine Specifications	Value/Detail
1	Bore Diameter (D), mm	92
2	Connecting Rod Length, mm	147
3	Stroke Length (L), mm	84.23
4	Clearance, mm	1.15
5	Compression Ratio	8.82
6	Engine Speed (N), rpm	1500
7	Fuel	IsoOctane
8	Stoichiometric Air Fuel Mass Ratio	15.0336
9	The diameter of the central electrode of the spark plug, mm	2
10	Spark Plug Duration, CA	20
11	Strength of Spark Plug, mJ	4.5

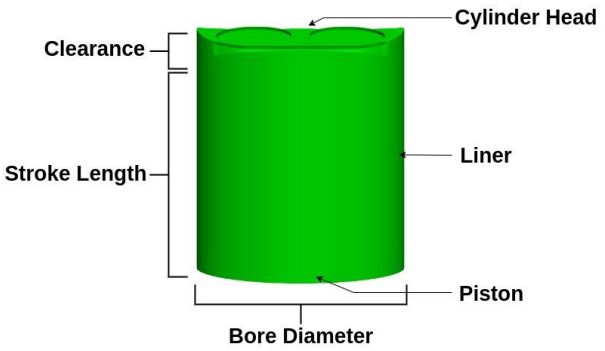

Figure 2. Computational domain for simulation of engine combustion.

2.2 Meshing Details

The computational domain was dynamically meshed using an automatic mesh motion solver with layered meshing. The mesh used in this study was identical to that of the KIVA-3V 4 valve model [14] used in OpenFOAM with the kivaToFoam grid conversion utility. Table 2 and Figure 3 provides information and a visual representation of the mesh at the beginning of the simulation, i.e. bottom dead centre (BDC).

Table 2. Mesh details at the start of the simulation

Mesh Statistics	Value/Detail
Cell type	Hexahedral
Number of cells	27,544
Number of points	30,742
Faces on piston	1,326
Faces on liner	2,710
Faces on the cylinder head	2,184
Internal faces	79,522
Maximum aspect ratio	34.032
Maximum skewness	3.739

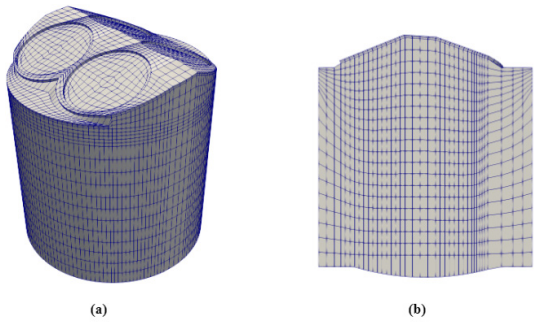

Figure 3. (a) Meshing of the engine cylinder during the start of the simulation. (b) Cross-sectional view of the meshing domain.

2.3 Governing Equations

EngineFoam solver [15] was used to simulate combustion in our study. The propagation of the flame front is represented by a progress variable. The progress variable can be denoted with the help of any quantity, like temperature or react mass fraction. In our case, we used temperature to calculate the progress variable.

$$c = \frac{T - T_u}{T_b - T_u} \tag{1}$$

The value of c lies between 0 and 1. Where 0 repre–sents a completely fresh air-fuel mixture, and 1 represents a completely burnt air-fuel mixture. The value of c between 0 and 1 represents an ongoing combustion reaction. The flame front is modelled using the transport equation, where a regress variable is defined as having exactly the opposite physical meaning of the progress variable.

$$b = 1 - c \tag{2}$$

$$\frac{\partial(\rho b)}{\partial t} + \nabla \cdot (\rho \cdot \tilde{u} \cdot b) - \nabla \cdot \left(\frac{\mu t}{Sct \times \nabla b} \right) = -\rho \cdot Sc \tag{3}$$

The reaction source term can be represented as

$$\rho \cdot Sc = \rho u \cdot Su \cdot \xi |\nabla b|$$

$$\frac{\partial(\rho b)}{\partial t} + \nabla \cdot (\rho \cdot \tilde{u} \cdot b) - \nabla \cdot \left(\frac{\mu t}{Sct \times \nabla b} \right) = \tag{4}$$

$$= -\rho u \cdot Su \cdot \xi |\nabla b|$$

For simulating the flow field, the RANS equation with the standard k-ε turbulence model was used. In the present study, our major focus was on flame pro–pagation and its effects on engine performance. Further details of continuity, momentum, turbulent kinetic energy and dissipation, internal energy, energy of state and chemical reaction can be found in [16, 17] as well as in the appendix section.

2.4 Initial and Boundary Conditions

During the beginning of the numerical simulation, the values of various parameters were specified, as shown in Table 3. The initial velocity is regarded to vary linearly, from zero at the cylinder head to the piston speed at the piston head. The liner and cylinder head were assumed to have no-slip conditions. The boundary layers were presumed to be turbulent and followed the law-of-the-wall velocity profile to aid in calculating heat and momentum losses. At the onset of the simulation, the air-fuel mixture was assumed to be evenly distributed throughout the cylinder and at rest.

Table 3. Values of different parameters during the start of the simulation

Parameter	Initial Value
Turbulent thermal diffusivity (αt)	0 m^2/s
Regress variable (b)	1
Turbulent kinetic energy dissipation rate (ε)	450 m^2/s^2
Turbulent kinetic energy (k)	4 m^2/s^2
Turbulent viscosity (μ_t)	0 m^2/s
Laminar flame speed (Su)	0.4 m/s
In-cylinder pressure (p)	1.9 bar
Internal temperature of the cylinder (T)	600 K
Temperature at the walls (T)	450 K
Flame wrinkling factor (ξ)	1

2.5 Numerical Schemes and Solver

The governing equations were discretised using the schemes mentioned in Table 4. More details of the schemes can be found in [18].

Table 4. Discretisation schemes used in the present simulation

Mathematical term	Discretisation scheme
Time derivative (∂/∂t, ∂^2/∂^2t)	Euler
Gradient (∇)	Gauss linear
Divergence (∇)	Gauss upwind, gauss linear, gauss linear limited
Laplacian (∇^2)	Gauss linear limited corrected
Point-to-point interpolation of values	Linear
Component of gradient normal to a cell face	Limited corrected

The PIMPLE (Pressure Implicit with Splitting of Operators Multi-Pressure-Linked Equations) algorithm was used to solve the discretised equations. Combining the SIMPLE and PISO algorithms, this algorithm is ideally adapted for solving turbulent phenomena. In the current simulation, the value of correctors for the PIMPLE algorithm is set to 2, corresponding to the number of times the algorithm solves the pressure and momentum in each time step. The value of non-orthogonal correctors is set to 1. In the current simulation, the moment predictor was utilised. The momentum predictor is a first approximation of the velocity field obtained from the solution of a momentum equation assembled with the previous time-step pressure field.

The absolute convergence criterion (tolerance) for various parameters is listed for the current simulations in Table 5.

Table 5. Converging criteria specified in the present simulation

Parameter	Tolerance
Pressure (p)	10^{-6}
Density (ρ)	10^{-5}
Velocity (U)	10^{-5}
Flame wrinkling factor (ξ)	10^{-5}
Regress variable (b)	10^{-5}
Turbulent kinetic energy dissipation rate (ε)	10^{-5}

The progression of the simulations was measured in terms of crank angle, with the bottom dead centre (BDC) at -180° and the top dead centre (TDC) at 0°. To precisely capture the flame propagation, the time step was maintained at 0.25° and decreased to 0.025° at the ignition's onset. The time steps met the CFL criteria effectively.

2.6 Validation

Figure 4 shows the comparison of the simulation with the findings of Anetor et al. [16]. Initial pressure and temperatures were maintained at the same levels as specified above. The spark was given 15° before the top dead centre. Thus, we received pressure readings similar to the reference until the spark plug ignited. Following the ignition, there seemed to be pressure value fluctuations with a maximum error of 11.69%, which was still within the permitted error margins. Besides

this, the numerical schemes used have been previously validated in [19, 20, 21].

3. RESULTS

Simulations were conducted for the engine's compre–ssion and power strokes (-180° to 180°) to understand the effect of spark plug position and spark timing.

3.1 Effect of spark plug position on single spark engine

The variation in the position of the spark plug was analysed by placing the spark plug at four different positions, i.e. 0.03 m, 0.02 m, 0.01 m and 0 m from the centre of the engine cylinder as depicted in Figure 5, adapted from [22].

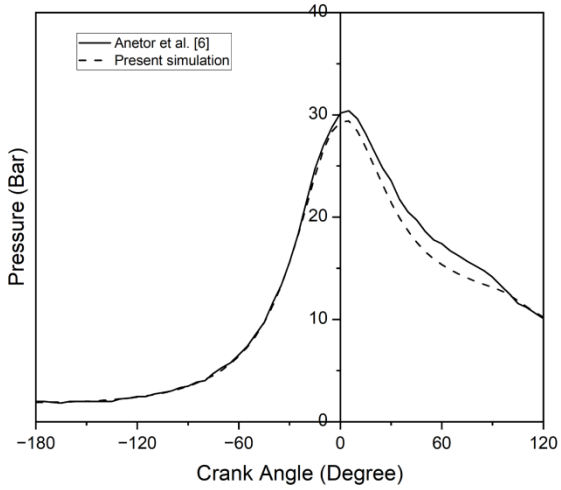

Figure 4. Comparison of in-cylinder pressure of present simulations with the results of Anetor et al. [9]

The ignition timing for all the cases was kept constant at 25° before TDC. Figure 6 depicts the in-cylinder pressure vs. crank angle for the four different spark plug locations. When the spark plug is positioned in the centre of the engine cylinder, a peak pressure of slightly more than 40 bar is recorded. The peak pressure drops when the spark plug goes farther from the centre. The reason behind this drop in pressure is associated with flame propagation, which is explained below.

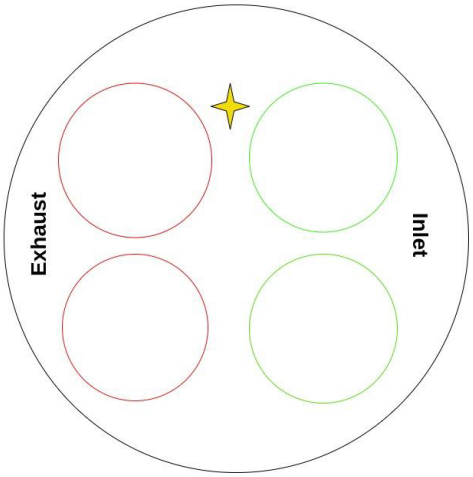

Figure 5. The spark plug placed between the exhaust and inlet valves.

Indicated Power (IP) is another parameter that we used to analyse engine performance. As IP is directly related to Indicated Efficiency (IE) and inversely pro–portional to Indicated Specific Fuel Consumption (ISFC), the greatest IP corresponds to the highest IE and lowest ISFC. IP was derived from indicated mean effective pressure (IMEP) using the formula:

$$IP(kW) = \frac{IMEP(bar) * L * \pi * D^2 * N * 100}{240 * n} \quad (5)$$

Here, the value of n is 2 for a four-stroke engine. IMEP signifies average pressure over an engine cycle. Thus, it was calculated using the p-v diagram of the compression and power stroke. A p-v diagram for the spark plug position 0.03 m from the centre is shown in Figure 7. The diagram illustrates the pressure and disp–lacement volume for compression and power stroke, while the intake and exhaust strokes were not taken into consideration. The area enclosed by the curve is equi–valent to the product of volume and IMEP. Table 6 displays the I.P. variance for different spark plug locations. It can be inferred that the spark plug posi–tioned in the middle of the engine cylinder achieves the maximum I.P.

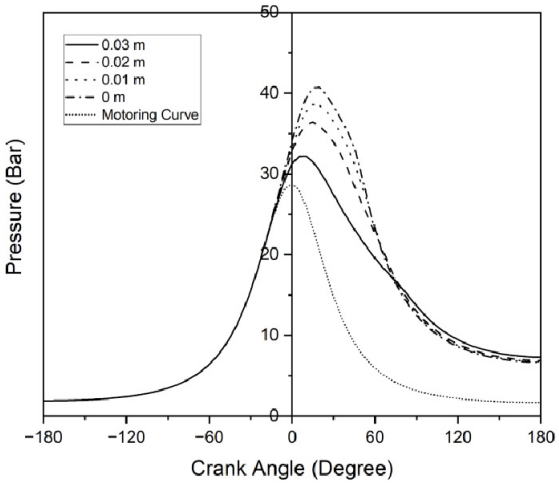

Figure 6. Pressure (Pa) vs. crank angle (degree) for diffe–rent positions of the spark plug in the single-spark engine.

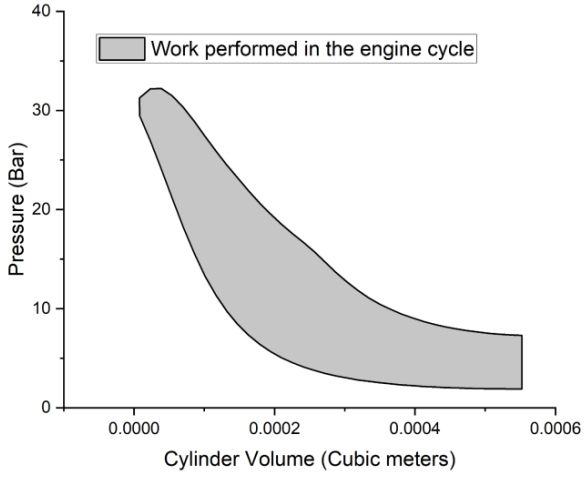

Figure 7. Pressure vs. displacement volume for compres-sion and power stroke in the single spark engine cylinder. Spark plug position at 0.03 m from the centre.

Table 6. Indicated Power for different positions of spark plug

Distance from the centre (m)	Indicated Power (kW)
0.03	6.85
0.02	7.90
0.01	8.31
0	8.61

The results demonstrate that the optimum engine performance is achieved when the spark plug is positioned in the cylinder's centre. This can be explained by the even flame propagation and combustion that occurs when the spark is positioned in the geometric centre of the combustion chamber. Any position other than the centre of the engine cylinder produces an uneven flame, hence decreasing engine performance. Figures 8(a) and 8(b) depict flame propagation for spark plugs located 0.03m from the centre and at the centre, respectively. When the ignition is initiated at -25° for both cases, the flame covers the entire engine cylinder at 50° for the case where the spark plug is positioned in the centre, unlike the position away from the centre. This demonstrates that flame propagation triggered by a spark plug at the engine's centre results in more rapid combustion than a spark initiated away from the engine's centre.

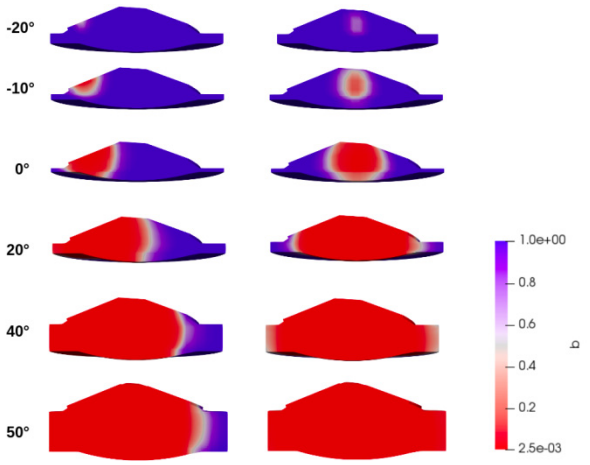

Figure 8. Flame propagation for different spark plug positions. (a) Spark plug at 0.03 m from the centre. (b) Spark plug at the centre of the engine cylinder.

3.2 Effect of spark time on the single-spark engine

For the single-spark engine, the spark timing was changed between 5° and 25° before TDC while maintaining the spark plug in the middle of the engine cylinder. It was noted that the pressure within the cylinder increased as one moved away from the TDC. The spark plug ignited 25° before TDC recorded the highest peak pressure of over 40 bar, as depicted in Figure 9. Similarly, Table 7 shows a rise in I.P. as we spark away from the TDC.

The results of this case study demonstrate that optimal engine performance is attained when the spark plug ignites significantly sooner in the compression stroke. This provides ample time for the flame front to propagate, i.e., the combustion process. Figure 10 illustrates an approximately 25° earlier completion of the combustion process for a -25° case than for a -5° case. This results in increased pressure and temperature, which is supported by the piston that continuously compresses the air-fuel mixture. However, it is necessary to determine the optimal spark timing, as igniting significantly earlier can lead to knocking due to a rapid increase in pressure and temperature.

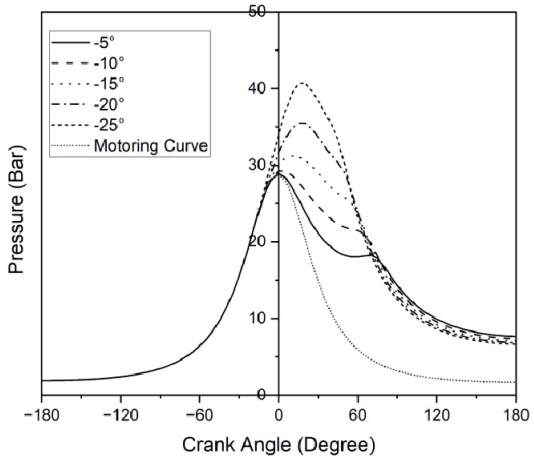

Figure 9. Pressure (Pa) vs crank angle (degree) for different spark timings in a single spark engine

Table 7. Indicated Power for different spark timings of spark plug

Crank Angle	Indicated Power (kW)
-5°	5.94
-10°	6.61
-15°	7.30
-20°	7.98
-25°	8.61

3.3 Effect of spark plug position on twin-spark engine

We attempted to determine the impact of spark plug configurations on a twin-spark engine. Even flame propagation was ensured by positioning the spark plugs in symmetrically opposite positions between the inlet and exhaust valves, as shown in Figure 11. Considering the results of a single spark engine, the spark plugs were ignited simultaneously 25° before TDC. Three hypothetical spark plug positions for computational simulations were analysed: 0.02 m, 0.01 m, and 0.005 m from the engine's centre.

Figure 12 and Table 8 demonstrate little difference in performance between the three positions. However, the intermediate position (0.01 m) produced slightly higher in-cylinder peak pressure and indicated power than the other two configurations.

This behaviour is explicable by the flame propagation and flame front collision phenomena. When spark plugs are positioned 0.02 m from the centre, as depicted in Figure 13(c), the flame fronts have to travel a greater distance to reach the centre and merge, as shown in Figure 13(c) at 10°. Due to the increasing volume of the engine cylinder after 0°, the flame gets weaker as it moves towards the centre. This decreases cylinder pressure and power compared to the 0.01 m spark plug position, as shown in Figure 12 and Table 8. However, a decrease in pressure and temperature can also be

observed in Figure 12 and Table 8 when spark plugs are positioned too close at a distance of 0.005 m from the engine's centre. Even though the flame front has to travel a very short distance to reach the centre of the engine cylinder, the flame fronts collide at a very early stage, as depicted in Figure 13(a) at -10°, thus resulting in lower in-cylinder peak pressure and power. This causes irregular flame propagation and decreased combustion efficiency. Therefore, the optimal place–ment of twin spark plugs in the engine requires a ba–lance between flame front propagation and collision, such as the case of a spark plug positioned 0.01m from the centre when flame collides at 0°, as illustrated in Figure 13(b).

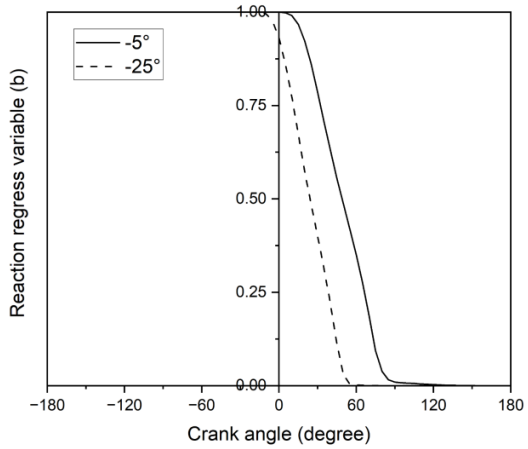

Figure 10. Reaction regress variable (b) vs crank angle (degree) for spark ignition angle of -25° and -5°.

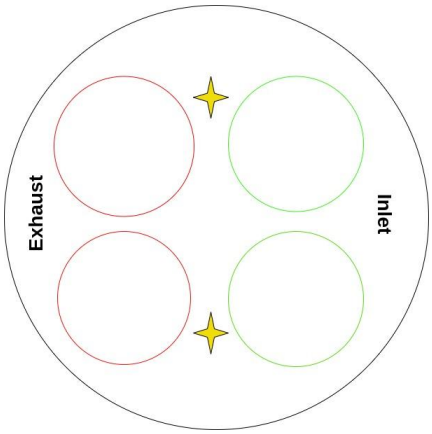

Figure 11. The spark plugs are placed at symmetrically opposite positions between the exhaust and inlet valves.

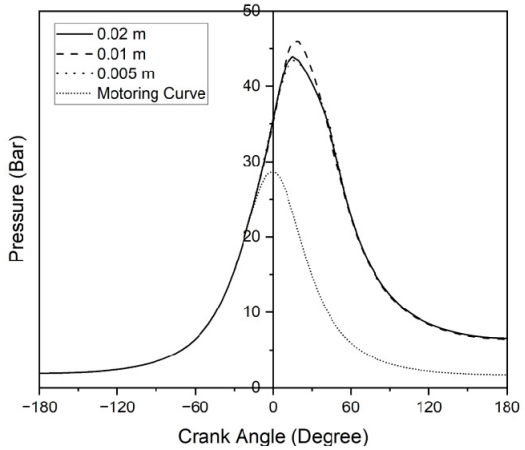

Figure 12. Pressure (Pa) vs. crank angle (degree) for different positions of the spark plug in a twin-spark engine.

Table 8. Indicated power (kW) for varying positions of spark plugs in twin spark engine

Distance from the centre (m)	Indicated Power (kW)
0.02-0.02	8.90
0.01-0.01	9.0
0.005-0.005	8.90

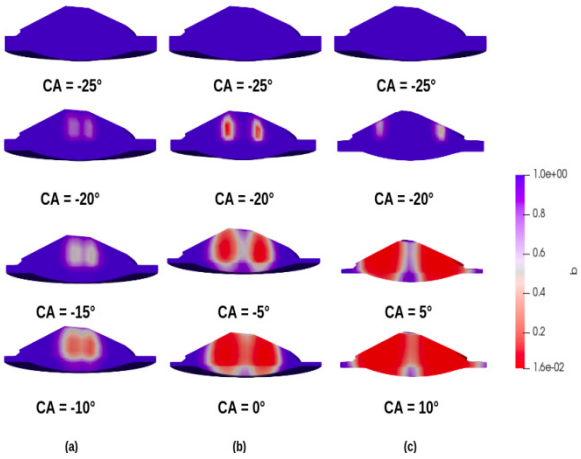

Figure 13. Collision of flame fronts at different time steps for different positions of twin spark plugs. The three different positions of spark plugs from the centre are (a) 0.005 m, (b) 0.01 m, (c) 0.02 m.

3.4 Effect of spark time in twin spark engine

The variation in spark timings was investigated by ma–intaining the spark timing of one spark plug at -25° before TDC and varying the spark timing of the second spark plug between -5° and -25°, with a 5° interval. The spark plugs were positioned at 0.01 m for optimal placement results.

After simulating the combustion within the cylinder at various spark timings, it was determined that the spark configuration of -5° and -25° produced the maximum peak pressure, as shown in Figure 14.

Figure 15 and Table 9 depict that the in-cylinder temperature and indicated power are also highest for the -25°: -5° configuration.

We obtain the best performance when the difference between the spark timing of two spark plugs is the greatest because the combustion and compression pro–cesses are applied for a prolonged period. When the first spark plug is ignited, the combustion process has sufficient time to spread, resulting in increased pressure and temperature, which are further increased by the piston, which consistently compresses the air-fuel mix–ture as it rises. Consequently, igniting the second spark plug adds more energy to the already heated and compressed air-fuel mixture, increasing cylinder pres–sure, temperature, and power.

Table 9. Indicated Power for different spark timings of spark plugs

Crank Angle	Indicated Power (kW)
-25°: -5°	10.01
-25°: -10°	9.37
-25°: -15°	8.79
-25°: -20°	8.70
-25°: -25°	8.99

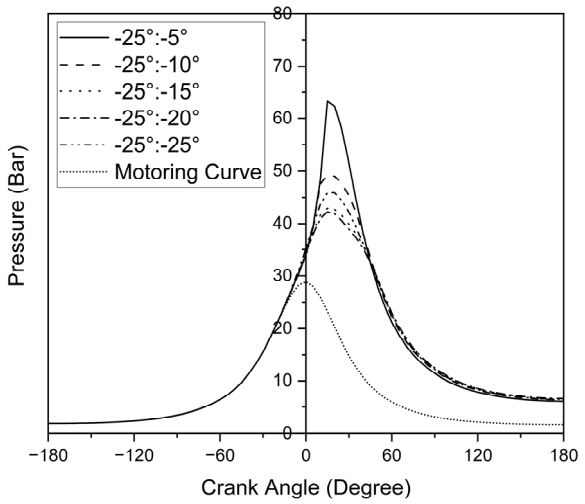

Figure 14. Pressure (Pa) vs. crank angle (degree) for different spark timings in a twin-spark engine

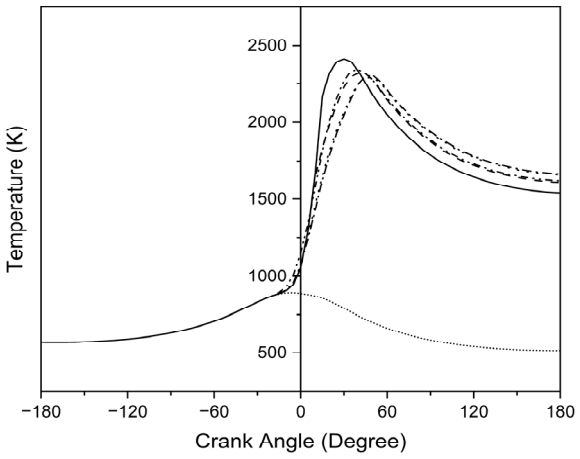

Figure 15. Temperature (K) vs. crank angle (degree) for different spark timings in a twin spark engine (Same legends as of Figure 14).

4. CONCLUSION

Computational simulations were performed to examine the effect of spark plug configuration variation (spark timing and position) in this study. The simulations were performed for both single and twin-spark engines. The following conclusion can be derived from the obtained simulation results.

1. As a result of the rapid combustion of the air-fuel mixture within the engine cylinder, optimal engine performance is achieved by a flame that spreads evenly.
2. Due to the extra time given for flame propagation, i.e. combustion, prior to the power stroke, an early ignition can increase cylinder pressure, tempe–rature, and power. However, the required pressure within the cylinder must be verified by the knocking tendency of the engine.
3. The timing of flame front collision in twin spark engines must be optimal. Neither too early, which would result in irregular flame propagation, nor too late, which would result in the collision of wea–kened flame fronts.
4. A higher difference in spark timings between the two sparks leads to higher in-cylinder pressure, tem–perature and power, which again needs to be kept in check with the knocking tendency of the engine.
5. A single-spark engine's highest pressure, tempe–rature, and power are obtained when the spark plug is positioned in the centre and ignited as early as possible while avoiding knocking.
6. The best results are obtained in a twin-spark engine when the spark plugs are optimally positioned and have the greatest spark timing difference.

REFERENCES

[1] Joshi, A., Borse, S.L., Alblawi, A. and Alshqirate, A.A.: Effect of spark plug position on performance of engine using openFoam. International Journal of Mechanical Engineering and Technology (IJMET) Vol. 9 Issue 11 (2018), pp. 114-120.

[2] Altin, I. and Bilgin, A.: A parametric study on the performance parameters of a twin-spark S.I. engine. Energy Conversion and Management 50 (2009), pp. 1902-1907.

[3] Joshi, A.R. and Borse, S.L.: Study of The Effect of Spark Advance, Engine Speed Variation and Number of Spark Plugs on Engine Performance Using CFD Software. Journal of Ocean, Mechanical and Aerospace Science and Engineering Vol 48 (2017), pp. 1-9.

[4] Gong, C., Sun, J., and Liu, F.: Numerical study of twin-spark plug arrangement effects on flame, combustion and emissions of a medium compression ratio direct-injection methanol engine. Fuel 279 (2020) 118427.

[5] Bailkeri, N., Prasad, K.S., and Rao, S.B.R.: Performance Study on Twin Plug Spark Ignition Engine at Different Ignition Timings. International Journal of Science and Research (IJSR) Vol. 2 Issue 8 (2013), pp. 231-236.

[6] Altin, I., Bilgin, A., Sezer, I.: Theoretical investiga-tion on combustion characteristics of ethanol-fueled dual-plug S.I. engine. Fuel 257 (2019), 116068.

[7] Yan, X., Feng, H., Zuo, Z., Jia, B., Zhang, Z. and Wu, L.: Research on the influence of dual spark ignition strategy at combustion process for dual cylinder free piston generator under direct injection. Fuel 299 (2021), 120911.

[8] Gong, C., Sun, J., Chen, Y. and Liu, F.: Numerical study of cold-start performances of a medium compression ratio direct-injection twin-spark plug synchronous ignition engine fueled with methanol. Fuel 285 (2021), 119235.

[9] Altin, I., Bilgin, A and Ceper, B.A.: Parametric study on some combustion characteristics in a natural gas fueled dual plug S.I. engine. Energy 139 (2017), pp. 1237-1242..

[10] Gong, C., Sun, J., Chen, Y. and Liu, F.: Numerical research on combustion and emissions behaviors of a medium compression ratio direct-injection twin-spark plug synchronous ignition methanol engine

under steady-state lean-burn conditions. Energy 215 (2021), 119193.

[11] Altin, I., Bilgin, A.: Quasi-dimensional mode–ling of a fast-burn combustion dual-plug spark-ignition engine with complex combustion chamber geomet–ries. Applied Thermal Engineering 87 (2015), pp. 678-687.

[12] Zhang, S. et al.: Numerical investigation the effects of the twin-spark plugs coupled with EGR on the combustion process and emissions characteristics in a lean burn natural gas S.I. engine. Energy 206 (2020), 118181.

[13] Kolambe, K.S. and Borse, S.L, Engine combustion simulation using openFoam.: International Engi–neering Research Journal (IERJ) Special Issue (2016), pp. 885-891

[14] Anthony A. A., KIVA-3V: A Block-Structured KIVA Program for Engines with Vertical or Canted Valves, Los Alamos National Laboratory, Los Alamos, New Mexico 87545 LA-13313-MS, UC-1412 (July 1997).

[15] Wadekar, S., engineFoam tutorial with different flame wrinkling (Xi) model, in: Proceedings of CFD with OpenSource Software, 2018, Edited by Nilsson. H., http://dx.doi.org/10.17196/OS_CFD# YEAR_2018.

[16] Anetor, L., Edward, E.O., Harris, K.: Simulation Studies of Combustion in Spark Ignition Engine using Openfoam. FME Transactions (2020) 48, pp. 787-799.

[17] Anetor, L., Edward, E.O., Odetunde, C.: Compa-rative analysis of combustion dynamics using three reaction source models. Australian Journal of Mec–hanical Engineering (2021).

[18] Christopher J. Greenshields, OpenFOAM.: The Open Source CFD Toolbox Programmer's Guide, Version 3.0.1, OpenFOAM Foundation Ltd, December 2015.

[19] Jasak, H. and Gosman, A.D.: Automatic resolution control for the Finite Volume Method. Part 1: A-posteriori error estimates, Numerical Heat Transfer, Part B, 38(3) (September 2000), pp. 237–256.

[20] Jasak, H., Gosman, A.D.: Residual error estimate for the Finite Volume Method, Int. Journal of Numerical Methods and Fluids 39 (2001), pp. 1-9.

[21] Weller, H.G., Tabor, G., Jasak, H.: and Fureby, C.: A tensorial approach to computational continuum mechanics using object orientated techniques, Computers in Physics 12(6) (1998), pp. 620-631.

[22] F., Claudio, Bianchi G.M., Corti, E. and Fantoni S.: Evaluation of the effects of a Twin Spark Ignition System on combustion stability of a high performance PFI engine, in: Processings of 69th Conference of the Italian Thermal Engineering Association, 10-13.09.2014, Milan, pp. 897-906.

NOMENCLATURE

c	Progress variable
Tu	Unburned gas temperature (K)
Tb	Burned gas temperature (K)
b	Regress variable
ũ	Filtered velocity of flame (m/s)
Sc	Reaction source term (net rate of production or consumption of species due to chemical reactions)
Sct	Turbulent Schmidt number (ratio of momentum diffusivity to scalar diffusivity in a turbulent flow)
Su	Laminar flame speed (m/s)

Greek symbols

ρ	Mean gas density (kg/m^3)
ξ	Wrinkling factor (ratio of turbulent flame velocity to laminar flame velocity)
ρu	Density of unburned mixture (kg/m^3)

APPENDIX

Continuity Equation:

$$\frac{\partial(\rho m)}{\partial t}+\nabla\cdot(\rho m\vec{u})+\nabla\cdot\left[\rho D\nabla\left(\frac{\rho m}{\rho}\right)\right]+\rho cm$$

Here ρ_m is the density of species m
ρ is the total mass density
$\vec{u}$ is fluid velocity
D is the coefficient of diffusion

ρcm is the source term due to chemistry

Summing all the species results in

$$\frac{\partial\rho}{\partial t}+\nabla\cdot(\rho\vec{u})+0$$

Momentum Equation:

$$\frac{\partial(\rho u)}{\partial t}+\nabla\cdot(\rho\vec{u}\vec{u})=-\nabla p-\nabla\left(\frac{2}{3}\rho\right)+\nabla\cdot\sigma+\rho\vec{g}$$

Here, p is fluid pressure.
σ stress tensor is Newtonian in form,

$$\sigma=\mu eff\left[\nabla\vec{u}+(\nabla\vec{u})^{\tau}\right]+\lambda\nabla\cdot\vec{u}I$$

Turbulent Kinetic Energy and Dissipation Models:

$$\frac{\partial(\rho k)}{\partial t}+\nabla\cdot(\rho\vec{u}k)=-\left(\frac{2}{3}\rho k\right)\nabla\cdot\vec{u}+\sigma:\nabla\vec{u}+$$
$$+\nabla\left[\left(\frac{\mu eff}{Pr_k}\right)\nabla k\right]-\rho\varepsilon$$

Here, k is turbulent kinetic energy
ε is the dissipation rate of k

$$\frac{\partial(\rho\varepsilon)}{\partial t}+\nabla\cdot(\rho\vec{u}\varepsilon)=-\left(\frac{2}{3}c_{\varepsilon 1}-c_{\varepsilon 3}\right)\rho\varepsilon\nabla\cdot\vec{u}+$$
$$+\nabla\left[\left(\frac{\mu eff}{Pr_{\varepsilon}}\right)\nabla\varepsilon\right]+\frac{\varepsilon}{k}\left[c_{\varepsilon 1}\sigma:\nabla\vec{u}-c_{\varepsilon 2}\rho\varepsilon\right]$$

Here, $\frac{\partial(\rho k)}{\partial t}$ represents convection of turbulence by the resolved velocity field.
$\nabla\cdot(\rho\vec{u}k)$ convection of turbulence by the resolved velocity field.
$-\left(\frac{2}{3}\rho k\right)\nabla\cdot\vec{u}$ is a compressibility term
$\sigma:\nabla\vec{u}$ represents the production of turbulence by shear
$\nabla\left[\left(\frac{\mu eff}{Pr_k}\right)\nabla k\right]$ represents self-diffusion with $\frac{\mu eff}{\rho}$ as diffusivity.
$\rho\varepsilon$ is the decay of turbulence into kinetic energy.

Equations of State:

The equations are assumed to be those of an ideal gas mixture.

$$p = R_o T\sum_m(\rho_m / W_m)$$

$$I(T) = \sum_m(\rho_m/\rho)I_m(T)$$

$$c_p(T) = \sum_m(\rho_m/\rho)c_{pm}(T)\cdot\frac{C_0}{pmR_0} = a_{1m} + $$
$$+a_{2m}T_m + a_{3m}T_m^2 + a_{4m}T_m^3 + a_{5m}T_m^4 + h_m(T) =$$
$$= I_m(T) + R_0T/W_m$$

$$\frac{s_m^0}{R_0} = a_{1m}\ln T_m + a_{2m}T_m + \frac{a_{3m}}{2}T_m^2 + \frac{a_{4m}}{2}T_m^3 +$$
$$+\frac{a_{5m}}{2}T_m^4 + a_{7m}$$

Here, R_0 is the universal gas constant
W_m is the molecular weight of species m
$I_m(T)$ the specific internal energy of species m
c_{pm} is specific heat coefficient at constant pressure
s^0 is specific entropy

Chemical Reaction:

$$\sum_m a_{mr}X_m == \sum_m b_{mr}X_m$$

Here, X_m is one mole of species m
a_{mr}, b_{mr} is integral stoichiometric coefficients for reaction r.

$$\sum_m(a_{mr} - b_{mr})W_m = 0$$

Kinetic reaction r proceeds at a rate ω_r which is

$$\omega_r = k_{fr}\prod_m(\rho_m/W_m)^{a'_{mr}} -$$
$$-k_{br}\prod_m(\rho_m/W_m)^{b_{mr}}$$
$$k_{fr} = A_{fr}T^{\varepsilon f_r}\exp(-E_{fr}/T)$$
$$k_{br} = A_{br}T^{\varepsilon b_r}\exp(-E_{br}/T)$$

Here, E_{fr} and E_{br} are activation temperatures.

$$K_c^r(T) = \prod_m(\rho_m/W_m)^{(b_{mr}-a_{mr})}$$

where $K^r_c(T)$ is concentration equilibrium constant.

$$\rho_m^c = W_m\sum_m(a_{mr} - b_{mr})\omega_r$$
$$Q^c = \sum_r Q_r\omega_r$$

Here, Q^c is chemical heat release

$$Q_r = \sum_m(a_{mr} - b_{mr})\left(\delta h_f^0\right)_m$$

Here $(\delta h_f^0)_m$ is the heat of formation of species m at absolute temperature zero.

$$\mu = \mu_{air} + c_\mu k^2/\varepsilon$$

$$\lambda = A_3\mu$$

$$K = \frac{\mu c_p}{Pr}$$

$$D = \frac{\mu}{\rho S_c}$$

Here c_μ is the empirical constant with a value of 0.09.
The Sutherland formula used for μ_{air} is

$$\mu_{air} = \frac{A_1T^{3/2}}{T + A_2}$$

Here, A_1, A_2 are constants
A_3 is taken as -⅔ for turbulent flow
Pr is Prandalt number
Sc is Schmidt number

НУМЕРИЧКО ИСПИТИВАЊЕ УТИЦАЈА КОНФИГУРАЦИЈЕ СВЕЋИЦА НА ПЕРФОРМАНСЕ У ЦИЛИНДРУ МОТОРА

Б. Мехул, П. Ранџан, А.К. Шукла

Нумеричко испитивање сагоревања у моторима са једном и двоструком варницом је извршено да би се проучавао утицај свећице, положаја и времена варнице на перформансе мотора. Побољшање перформанси мотора је једно од примарних области истраживања аутомобилске индустрије. Сходно томе,

резултати студије се могу искористити за оптимизацију конфигурације мотора како би се постигле максималне перформансе. Истраживање је спроведено коришћењем софтвера отвореног кода заснованог на ограниченом волумену, ОпенФОАМ, за рачунарске симулације. Симулације су спроведене коришћењем КсиЕнгинеФОАМ решавача са транспортном једначином за моделовање фронтова пламена. Стандардни к-ε модел турбуленције је коришћен за предвиђање параметара турбуленције. Симулација је спроведена за компресију и ход снаге (угао курбле између -180° и 180°), уз претпоставку равномерне дистрибуције смеше ваздуха и горива унутар цилиндра мотора са 4 вентила. Симулације су спроведене за четири случаја, укључујући варијације у положају и времену свећица у моторима са једном и двоструком варницом. Према резултатима симулација, мотор са једном варницом даје најбоље перформансе када се свећица рано упали и постави у центар цилиндра. Када се постави на оптималан положај одређен кретањем пламена и сударом, мотор са две свећице даје најбоље перформансе при највећој разлици између времена паљења две свећице.